END

MICROCOPY RESOLUTION TEST CHART

NATIONAL BUREAU OF STANDARDS-1963-A

The Effect of Noisy Reflection Data on an Inverse Method for Determining the Structure of a Layered Ocean Bottom

AD A131976

A Paper Presented at the
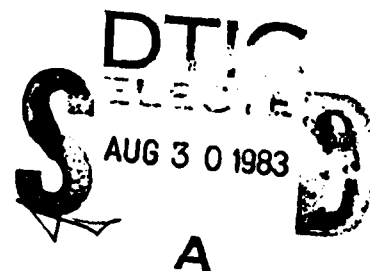105th Meeting of the Acoustical Society
of America, 11 May 1983, Cincinnati, Ohio

David J. Thomson
Peter D. Herstein
Surface Ship Sonar Department

Naval Underwater Systems Center
Newport, Rhode Island / New London, Connecticut
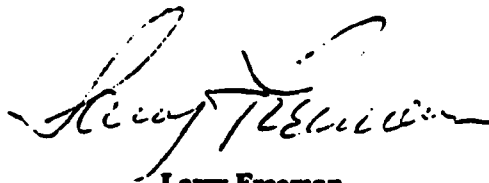
DTIC
ELECTE
AUG 3 0 1983

A

DTIC FILE COPY

83 08 29 077

Preface

This document was prepared under NUSC Project No. A65000, *EVA Support for Shipboard Sonar* (U), Principal Investigator, B. F. Cole (Code 3302). The sponsoring activity is the Naval Sea Systems Command, C. D. Smith (NAVSEA 63R), Director. Funding is provided under Program Element No. 62759N, Subproject Program No. SF 59-552A, F. R. Romano (NAVSEA 63R3), Manager.

Reviewed and Approved: 18 July 1983

Larry Freeman
Surface Ship Sonar Department

The authors of this document are located at the
New London Laboratory, Naval Underwater Systems Center,
New London, Connecticut 06320.

Dr. D. J. Thomson is an exchange scientist from the
Defence Research Establishment Pacific,
Victoria, B.C., V0S 1B0, Canada.

1. REPORT NUMBER TD 6947	2. GOVT ACCESSION NO.	3. RECIPIENT'S CATALOG NUMBER
4. TITLE (and Subtitle) THE EFFECT OF NOISY REFLECTION DATA ON AN INVERSE METHOD FOR DETERMINING THE STRUCTURE OF A LAYERED OCEAN BOTTOM		5. TYPE OF REPORT & PERIOD COVERED
		6. PERFORMING ORG. REPORT NUMBER
7. AUTHOR(s) David J. Thomson* and Peter D. Herstein *Exchange scientist from Defence Research Establishment Pacific, Victoria, B. C., Canada		8. CONTRACT OR GRANT NUMBER(s)
9. PERFORMING ORGANIZATION NAME AND ADDRESS Naval Underwater Systems Center New London Laboratory New London, CT 06320		10. PROGRAM ELEMENT, PROJECT, TASK AREA & WORK UNIT NUMBERS
11. CONTROLLING OFFICE NAME AND ADDRESS Naval Sea Systems Command Washington, DC 20362		12. REPORT DATE 18 July 1983
		13. NUMBER OF PAGES
14. MONITORING AGENCY NAME & ADDRESS (if different from Controlling Office)		15. SECURITY CLASS. (of this report) UNCLASSIFIED
		15a. DECLASSIFICATION / DOWNGRADING SCHEDULE

16. DISTRIBUTION STATEMENT (of this Report)

Approved for public release; distribution unlimited.

17. DISTRIBUTION STATEMENT (of the abstract entered in Block 20, if different from Report)

18. SUPPLEMENTARY NOTES

19. KEY WORDS (Continue on reverse side if necessary and identify by block number)

bottom reflection coefficient	inverse problem	numerical integration
Gaussian noise	plane waves	sediment sound-speed profile
geoacoustic model	sediment density profile	sediment structure
inversion algorithm	sediment impulse response	underwater acoustics

20. ABSTRACT (Continue on reverse side if necessary and identify by block number)

A basic inverse problem in underwater acoustics is the determination of the structure of the sea bed from a limited knowledge of its reflection coefficient. For many applications, an adequate model for studying the acoustic interaction is provided by the scattering of plane waves by a layered liquid medium. In contrast to formally exact solutions to this inverse scattering problem, Candel, et al., [J. Sound Vib. 68, 571-595 (1980)] developed an approximate scheme which is readily implemented numerically. Under the assumption of nonabsorptive media, the reconstruction of both sediment density and sound-speed profiles

DD, FORM 1473

20. (Cont'd)

cont →

is effected by the numerical integration of a system of four first-order differential equations requiring impulse response data for two distinct grazing angles. In this paper, the effect of additive noise on the inversion algorithm is examined for synthetic reflection data generated for a geoacoustic model of deep-sea sediments representative of the Hatteras Abyssal Plain.

THE EFFECT OF NOISY REFLECTION DATA ON AN
INVERSE METHOD FOR DETERMINING THE STRUCTURE OF A
LAYERED OCEAN BOTTOM

At low frequencies, sound waves propagating within the sea can readily penetrate the sea bed to considerable depths. Hence, proper interpretation of acoustic signals which penetrate the sea bottom requires a knowledge of the density and sound-speed profiles below the sea floor. A basic problem is the determination of the structure of the sea bed from a limited knowledge of the reflected waves. For many applications, an adequate model for studying this inverse problem is the scattering of plane acoustic waves by a one-dimensional inhomogeneous medium.

# THE EFFECT OF NOISY REFLECTION DATA ON AN INVERSE METHOD FOR DETERMINING THE STRUCTURE OF A LAYERED OCEAN BOTTOM

BACKGROUND

- **BURRIDGE (1980)**

- **NEWTON (1981)**

- **CANDEL, DEFILLIPI & LAUNAY (1980)**

- **THOMSON (1983)**

Viewgraph 1

Formal methods for solving one-dimensional inverse scattering problems are reviewed by Burridge (1980) and Newton (1981). Candel, Defillipi and Launay (1980) proposed an approximate scheme which is readily implemented numerically. An important feature of the Candel, et al., approach is the separate recovery of both density and sound-speed profiles from two band-limited impulse responses associated with different grazing angles. The inversion of noise-free reflection data using their algorithm has been presented elsewhere by Thomson (1983). However, measured sediment reflection data will always contain some level of noise because of ambient noise in the ocean and data processing limitations. Today we will present the results of a study of the effects of inverting simulated reflection data containing various levels of Gaussian noise.

Model for One-dimensional Inverse Method
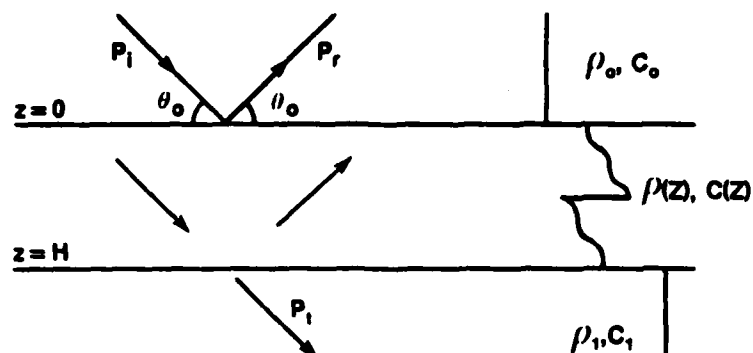
- PLANE WAVES
- HORIZONTAL LAYERING
- LIQUID LAYERS
- ZERO ABSORPTION

Viewgraph 2

In the mathematical model to be considered, the horizontally layered region $0 < z < H$ is occupied by an inhomogeneous liquid having arbitrary variation of density $\rho(z)$ and sound-speed $c(z)$. The half-spaces $z < 0$ and $z > H$ are homogeneous. All regions are assumed to be non-absorbing.

A plane acoustic wave, initially propagating downward at the grazing angle θ_0 encounters the inhomogeneous medium at $z = 0$. Within $0 < z < H$, the incident wave is partially reflected and a reflected wave is returned to the region $z < 0$. In $z > H$, only a transmitted wave continues to propagate.

Frequency Response of the Reflection Coefficient as a Non-linear Fourier Transform

- $R(f,\theta) = -\int_0^H g(z) \exp\left[2i \int_0^z k_z(s)\,ds\right]\,dz$

- $g = \dfrac{1}{2Y_z}\dfrac{dY_z}{dz} = \dfrac{1}{2}\dfrac{d}{dz}\ln(Y_z)$

- $Y_z = (k_z/k)/(\rho c)$

- $k_z = (k^2 - k_x^2)^{1/2} = k\sin\theta$

Viewgraph 3

As a result of applying the forward scattering approximation to a local wave representation of the field, Candel, et al., derived an approximate form for the reflection coefficient R as a function of the frequency f and grazing angle θ. In the upper line, observe that R appears as a non-linear Fourier transform. The kernel of the transform, g, is one-half the logarithmic derivative of "longitudinal admittance", Y_z. Y_z is defined in terms of the z-component of the total wavenumber k. For a plane wave having wavenumber components k_x and k_z, Y_z is the ratio of the z-component of the particle velocity to the pressure (i.e., the longitudinal admittance).

Frequency Response of the Reflection Coefficient as a Standard Fourier Transform

$$\bullet \quad z^* = (2/k_o) \int_0^Z k_z(s)\,ds$$

$$\bullet \quad R(f,\theta) = -\int_0^{z^*(H)} g(z^*)\exp[2\pi i f z^*/c_o]\,dz^*$$

Time Response of the Reflection Coefficient determines the Relative Variation of Admittance

$$\bullet \quad r(t,\theta) = \int_{-\infty}^{\infty} R(f,\theta)\exp(-2\pi i f t)\,df$$

$$= -\frac{c_o}{2Y_z}\frac{dY_z}{dz^*}\bigg|_{z^*=c_o t}$$

Viewgraph 4

By a change of variable, the reflection coefficient can be written as a standard Fourier transform in the new depth coordinate z*. If we take the Fourier transform with respect to time in order to obtain the impulse response of the reflection coefficient, we arrive at the desired result that the impulse response at time, t, is related to the relative variation of longitudinal admittance, Y_z, at depth z* = c_ot.
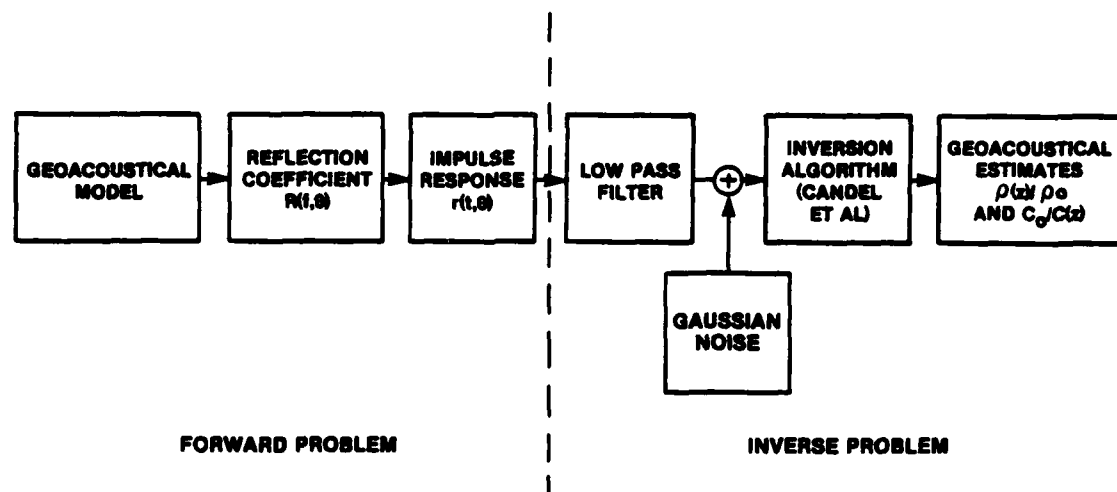
Algorithm to Recover Admittance Profile from a Single Impulse Response

- $dY_z/dz^* = -(2/c_o)r\ Y_z,\ Y_z(0) = \sin\ \theta_o/\ (\rho_o c_o)$

- $dz/dz^* = (2\ \rho c_o Y_z)^{-1},\ z(0) = 0$

Viewgraph 5

These equations represent Candel's, et al., non-iterative algorithm for determining admittance as a function of depth from a single impulse response. All that is required is the integration of a pair of first-order differential equations with appropriate initial conditions. Either $\rho(z)$ or $c(z)$ is required to be known in order to effect the inversion. Candel, et al., have shown that if two impulse responses corresponding to different grazing angles are available, then unique determination of both $\rho(z)$ and $c(z)$ is possible without any prior knowledge of either bottom profile. In this case, four differential equations have to integrated instead of two.

Simulation of Noisy Impulse Responses


```
GEOACOUSTICAL        REFLECTION        IMPULSE         LOW PASS            INVERSION         GEOACOUSTICAL
MODEL                COEFFICIENT       RESPONSE        FILTER    ⊕        ALGORITHM          ESTIMATES
                     R(f,θ)            r(t,θ)                               (CANDEL           ρ(z)/ρo
                                                                           ET AL)            AND Co/C(z)
```

GAUSSIAN
NOISE

FORWARD PROBLEM   INVERSE PROBLEM

Viewgraph 6

The simulation of noisy impulse responses for the inversion
algorithm is shown in this block diagram. For a given
geoacoustic model and incident grazing angle, the complex fre-
quency response R(f) is computed at 256 discrete equispaced
frequencies ranging from 0 to 127.5 Hz. The sequence is
extended to 1024 points by appending zero values. A fast
Fourier transform (FFT) is used to produce a bandlimited
impulse response r(t). This constitutes a solution to the
forward problem.

Each impulse response is convolved with a low-pass digital
filter having a cut-off frequency of 63.5 Hz. This is found
necessary to inhibit Gibbs oscillations due to the truncation
of the sampled frequency response. Zero-mean, Gaussian noise
is added to each point of the filtered time sequence. Two
"noisy" impulse responses, representing grazing angles 60°
and 90°, are supplied to the inversion algorithm.
Reconstructed estimates of the normalized density $\rho(z)/\rho_0$
and sound-speed $c_0/c(z)$ profiles are compared to the known
values comprising the geoacoustic model.

Hatteras Abyssal Plain Geoacoustic Model
(28° 30′ N, 70° 30′ W)
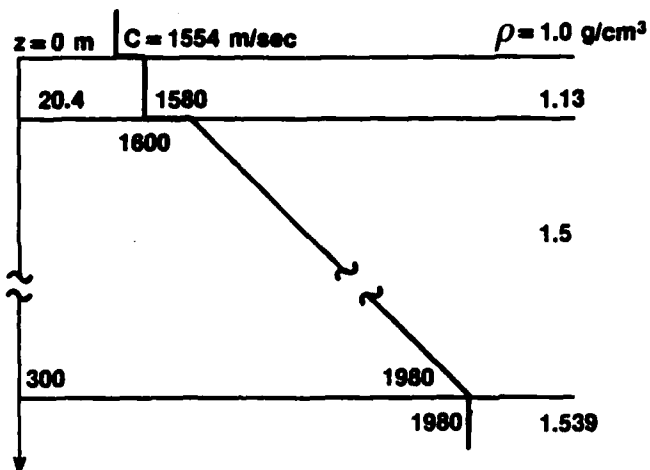
Viewgraph 7

The geoacoustic model used in the simulations is based on the interpretation of Herstein, Dullea and Santaniello (1979) for measurements made at a site in the Hatteras Abyssal Plain. Both density and sound-speed profiles exhibit discontinuities at layer boundaries. The upper layer is thin and iso-velocity. The deep layer is characterized by an upward refracting sound-speed gradient.

Definition of Signal-to-Noise Ratio (SNR)

- $SNR = 10 \log_{10}(I_s/I_n) \, dB$

- $I_s = (1/T) \int_{t_1}^{t_1+T} r^2(t) \, dt$

- $I_n = (1/T) \int_{t_1}^{t_1+T} n^2(t) \, dt \approx \sigma_n^2$

- $SNR = 10 \log_{10}(I_s/\sigma_n^2)$

GIVEN SNR, THEN $\sigma_n = I_s^{+1/2} 10^{-SNR/20}$

Viewgraph 8

In this simulation, the signal-to-noise ratio (SNR) in dB is defined as 10 $\log_{10}$ of the signal intensity divided by the noise intensity. The signal intensity is computed by integrating the square of the reflection impulse response over an appropriate time window and then dividing by the window length. The noise intensity is computed similarly over the noise series. Note that the intensity of the noise can be approximated by its variance. Hence, if the signal intensity is known, the variance of the noise required to simulate a desired SNR can be computed as shown in the bottom line.
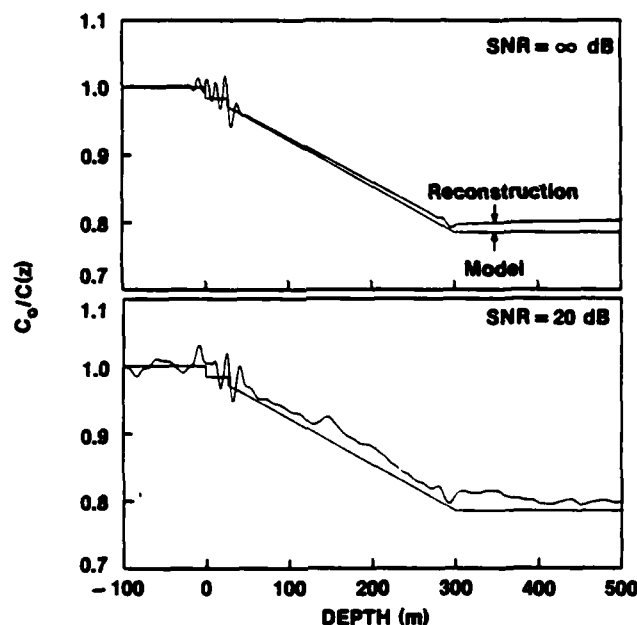
Simulated Impulse Responses
Grazing Angle θ = 60°
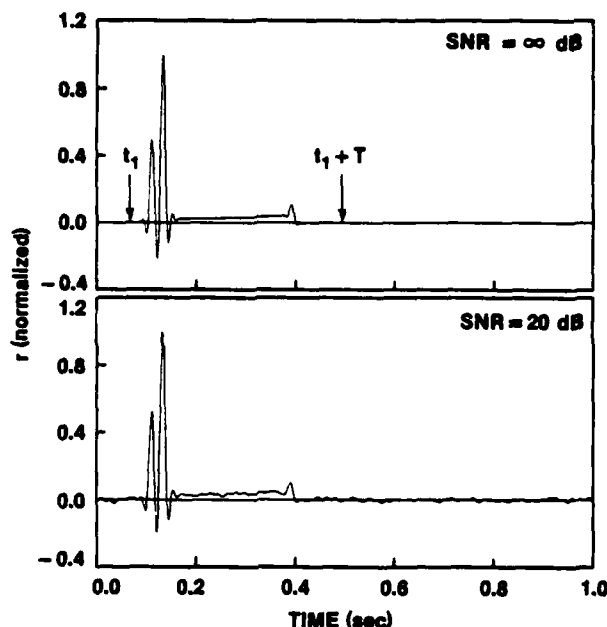
Viewgraph 9

This viewgraph shows examples of bandlimited reflectivity impulse responses generated for the Hatteras model for a grazing angle of 60°. The upper trace corresponds to the noise-free case. The lower trace corresponds to a signal-to-noise ratio of 20 dB determined for an appropriate time window, T. The three "pulses" observed in each response are associated with discontinuities in the density and/or sound-speed profiles at layer boundaries. Between the second and third "pulses" there appear continuous reflections arising from the positive sound-speed gradient of the deep layer. Similar responses are obtained for a grazing angle of 90°.

Reconstructed Sound-speed Profile Using Grazing Angles 60° and 90°

Viewgraph 10

Using bandlimited impulse responses for grazing angles 60° and 90°, Candel's, et al., inversion algorithm was used to obtain the reconstructed sound-speed profiles shown here. The sound-speed versus depth variations are presented in the form of acoustic refractive index profiles. For comparison, the Hatteras Abyssal Plain input model values are also indicated. The top comparison relates to the noise-free case. While the global agreement is excellent, the highest frequency present in the low-pass impulse responses is insufficient to resolve the refractive index within the thin upper layer of the model. The lower comparison shows the effect of adding noise at the 20 dB SNR level. Again, the global agreement is good but the local effects of the noise are evident. Note that the sound-speed gradient of the deep layer is accurately recovered in both cases.

Reconstructed Density Profile Using
Grazing Angles 60° and 90°
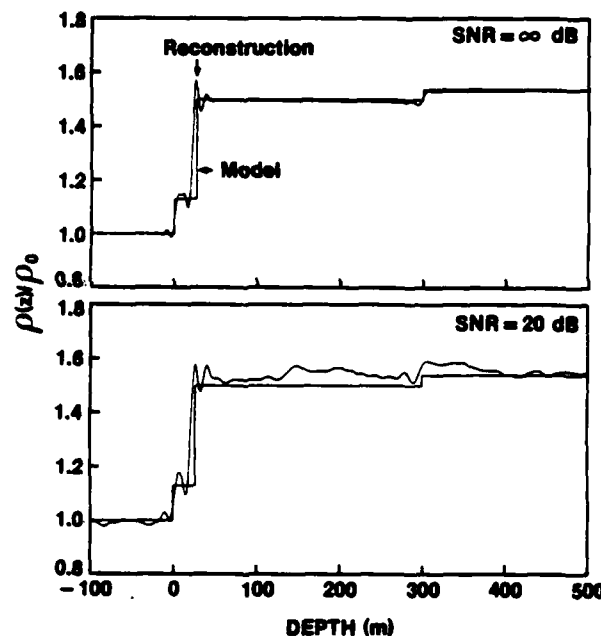
Viewgraph 11

The reconstructed density profiles normalized to the density in the region z < 0 are displayed next. As before, the top comparison is for the noise-free case and the lower comparison is for a 20 dB signal-to-noise ratio. These results show that the resolution of the density profile is better than that obtained for the refractive index profile. This improvement in resolution is due in part to the larger relative variation in density for the Hatteras model. Observe that even the density within the thin upper layer of the model is resolved.

Root Mean Square Error

$$E(SNR) = 100 \left\{ \frac{1}{N} \sum_{i=1}^{N} \left(\frac{\hat{X}_i(SNR) - X_i}{X_i} \right)^2 \right\}^{1/2}$$

X_i = TRUE

$\hat{X}_i$ = RECONSTRUCTED

ρ/ρ_0 = -------

C_0/C = _____
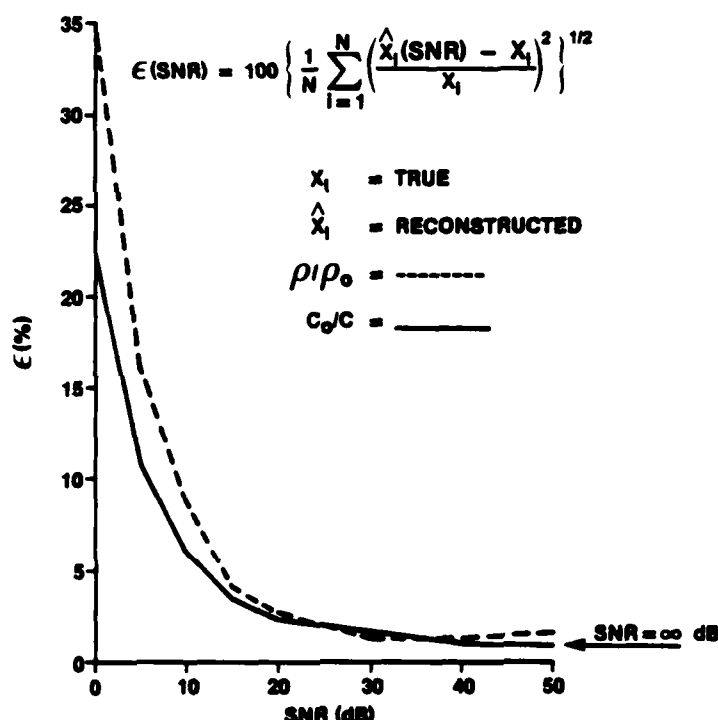
Viewgraph 12

A set of simulations was carried out as a function of signal-to-noise ratio. The effect of signal-to-noise ratio on the profiles reconstructed via Candel's, et al., inversion algorithm are presented in terms of a root mean square error measure. Each error value was determined by summing the squares of the relative differences between reconstructed and true profiles over the depth interval displayed in the previous Viewgraphs. Error measures are plotted for both normalized density and refractive index.

For signal-to-noise ratios greater than approximately 20 dB the errors differ only slightly from the error associated with the noise-free case. This nonzero error for the noise-free case arises since, first, the reconstructions are based on bandlimited impulse responses and, second, the inversion algorithm itself is based on a forward scattering approximation. For signal-to-noise ratios less than 15 dB, the errors increase rapidly. Note that the inversion remained stable (i.e., realizable) even for a signal-to-noise ratio of 0 dB. These results agree well with the results published recently by Schwetlick (1983) using other methods of profile inversion.

12

Signal-to-noise ratios of 15 dB have routinely been obtained for measurements of acoustic reflectivity at sea. This is particularly true for the high grazing angles, i.e., close ranges, appropriate for the implementation of Candel's, et al., inversion method. Replicate averaging or beamforming methods could be used to obtain further increases in signal-to-noise ratio.

We conclude that Candel's, et al., non-iterative algorithm is a viable method for geoacoustic models similar to the Hatteras Abyssal Plain model, provided adequate signal-to-noise ratios are available. An important feature of the algorithm is the recovery of both density and sound-speed profiles from just two bandlimited impulse responses. No prior knowledge of either profile is required for the inversion. Beyond this simulation, we intend to apply Candel's, et al., method to high signal-to-noise measurements of sea-bed reflection responses.

Thank you. Are there any questions?

REFERENCES

1. R. Burridge, "The Gelfand-Levitan, the Marchenko, and the Gopinath-Sondhi Integral Equations of Inverse Scattering Theory, Regarded in the Context of Inverse Impulse-Response Problems," Wave Motion, vol. 2, 1980, pp. 305-323.

2. S. M. Candel, F. DeFillipi and A. Launay, "Determination of the Inhomogeneous Structure of a Medium from Its Plane Wave Reflection Response, Part I: A Numerical Analysis of the Direct Problem" and "Part II: A Numerical Approximation," Journal of Sound and Vibration, vol. 68, 1980, pp. 571-595.

3. P. D. Herstein, R. K. Dullea and S. R. Santaniello, "Hatteras Abyssal Plain Low Frequency Bottom Loss Measurements," NUSC Technical Report 5781, Naval Underwater Systems Center, New London, CT, 1979.

4. R. G. Newton, "Inversion of Reflection Data for Layered Media: A Review of Exact Methods," Geophysical Journal of the Royal Astronomical Society, vol. 65, 1981, pp. 191-215.

5. H. Schwetlick, "Inverse Methods in the Reconstruction of Acoustical Impedance Profiles," Journal of the Acoustical Society of America, vol. 73, 1983, pp. 1179-1186.

6. D. J. Thomson, "The Determination of Material Properties of the Sea-Bed from the Acoustic Plane-Wave Reflection Response," Proceedings of the "Acoustics and the Sea-Bed" Conference, 6-8 April 1983, Bath, UK, ed. by N. G. Pace, Bath Univ. Press, 1983, pp. 41-49.

INITIAL DISTRIBUTION LIST

Addressee	No. of Copies
DARPA (TTO)	1
DARPA (CDR K. Evans)	1
CNO (OP-095;-098; CAPT E. Young, CDR. H. Dantzler, 952D	4
CNM (SPO PM-2; MAT-0723, -0724 (CAPT J. Harlett), -05 (R. Hillyer), -907 (L. L. Hill)	5
NAVELEX (R. Mitnick, J. Schuster, 612; R. Knudsen, PME-124)	3
NAVSEASYSCOM (SEA-63R; L. Kneesi,-63D; D. Porter,-63R; F.Romano,-63R; R. Farwell,-63R)	5
NAVPGSCOL	1
DWTNSRDC	1
NORDA (R. Lauer, 320; S. Marshall, 115; R. Martin, 110A; L. Solomon, 500; R. Gardiner, 520; E. Chiaka, B. Blumenthal, W. Worsley, R. Wheatly, 530; J.Matthews; G. Stanford; Library)	12
NOSC (R. Bolam, 7133; R. Albrecht, 7134; M. Pederson, D. Gordon, 712; J.R. McCarthy, 713, C. Persons, 7133; S. Sullivan, 1604; R. Smith; J. Lovett, G. Tunstall; Library)	11
NADC (J. Howard; B. Steinberg, P. Hass; Library)	4
NCSC	1
NSWC (R. Stevenson; M. Stripling; M. Stallard; Library)	4
NRL (O. Diachok, R. Dicus, 5160; J. Munson, 5100, W. Mosley, 5120; A. Eller, 5109; Library)	6
MPL (V.C. Anderson; F. Fischer; B. Williams)	3
NAVAIR (E. David, 370B; W. Parrigian, 370J)	2
NISC (H. Foxwell)	1
DTIC	2
ONR (R. Winokur, ONR-102B; CAPT E. Craig, T. Warfield, ONR-220; G. Hamilton, ONR-420; J. McKisic, ONR-4250A; P. Rogers, ONR-425UA; J. A. Smith; ONR-100; ONR-480)	9
DIA	1
CHESNAVFACENGCOM	1
ARL (Univ. of Texas) (P. Vidmar; K. Hawker; R. Koch; Library	4
ARL (Penn State Univ.) (S. McDaniel; D. McCammon; Library)	3
Courant Institute (D.C Stickler; Library)	2
SAI (C.W. Spofford, R. Greene)	2
Cornell University (H. Schwetlick)	1
Northwestern University (G. Kriegsmann)	1
Univ. of Denver (J.A. DeSanto, F. Hagin)	2
General Instrument Co. (R. Breton)	1
FWG (D. Wille)	1

Addressee	No. of Copies
CANADA	
DREP	20
DSIS (Microfiche Section, Report Collection)	3
DREA	1
ORAE Library (DMOR)	2
CDLS/L CDR	1
CDLS/W CDR	1
CMDO	1
DMRS	1
Commander Maritime Command (MC/ORD, SSO Ocean)	2
CFMWS	1
Maritime Headquarters Pacific (SSO Op Rsch)	1
DST(SE)3	1
DTA(M)3	1
RRMC (Dept. of Oceanography)	1
D Met Oc	1
Project Officer IEP ABCANZ-2, NOP 981, Pentagon	3
BRITAIN	
DRIC	3
AUWE	1
RAE	1
AUSTRALIA	
DRC	1
NEW ZEALAND	
DSE	1

END

FILMED

9-83

DTIC